JCB

Supplemental material

Hariri et al., https://doi.org/10.1083/jcb.201808119

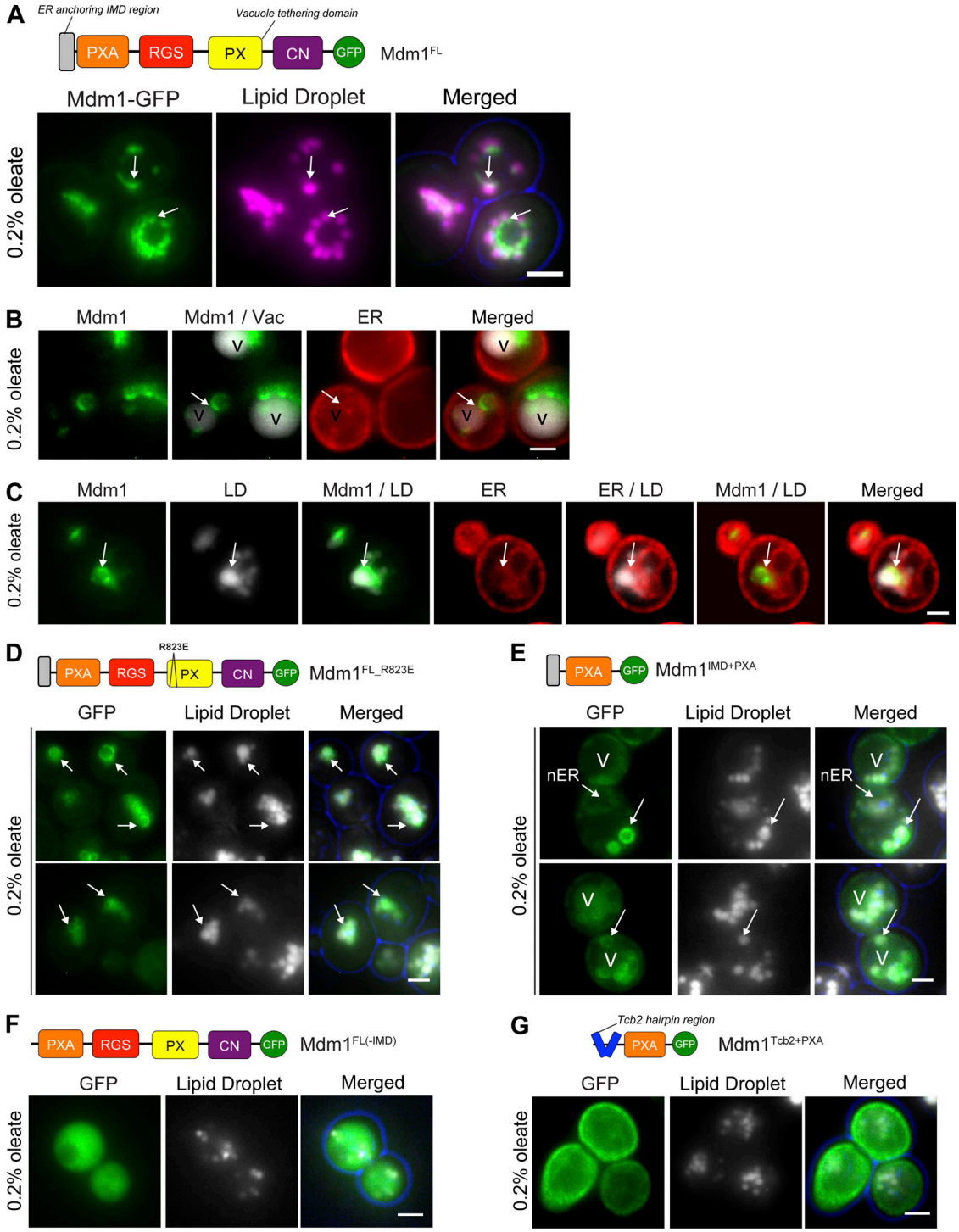

Figure S1. **Mdm1 binds lipid droplets via its N-terminal region. (A)** Light microscopy of yeast overexpressing GFP-tagged Mdm1 in the presence of 0.2% oleate. LDs (magenta) visualized by MDH staining. Arrows indicate LD-Mdm1 close association. Scale bar, 2 µm. **(B)** Light microscopy of yeast overexpressing GFP-tagged Mdm1 in the presence of 0.2% oleate. LDs (gray) visualized by MDH staining, and chromosomally tagging Ds-Red HDEL was used to label the ER. Arrows indicate the association between Mdm1 and ER-bound LDs. Scale bar, 2 µm. **(C)** Light microscopy of yeast overexpressing Mdm1 in the presence of 0.2% oleate. The vacuole (V) was visualized by using CMAC dye. Ds-Red HDEL marker was used to label the ER. Arrows indicate the close association between ER-anchored Mdm1 and the vacuole. Scale bar, 2 µm. **(D)** Light microscopy of yeast expressing GFP-tagged $Mdm1^{FL\_R823E}$, which lacks vacuole binding ability. Cells were treated with 0.2% oleate overnight, and LDs (gray) were visualized by using MDH. Arrows indicate ER rings around LDs. Scale bar, 2 µm. **(E)** Light microscopy of yeast expressing GFP-tagged truncated $Mdm1^{IMD+PXA}$. Cells were treated with 0.2% oleate overnight, and LDs (gray) were visualized by using MDH. Arrows indicate ER rings around LDs. Scale bar, 2 µm. **(F)** Light microscopy of yeast expressing GFP-tagged (soluble) Mdm1 lacking the IMD region. Cells were treated with 0.2% oleate overnight, and LDs (gray) were visualized by using MDH. Scale bar, 2 µm. **(G)** Light microscopy of yeast expressing GFP-tagged truncated Mdm1 with Tcb2 membrane-anchoring hairpin region instead of Mdm1 IMD domain. Cells were treated with 0.2% oleate overnight, and LDs (gray) were visualized by using MDH. RGS: regulator of G protein signaling, CN: C-terminal Nexin. Scale bar, 2 µm.

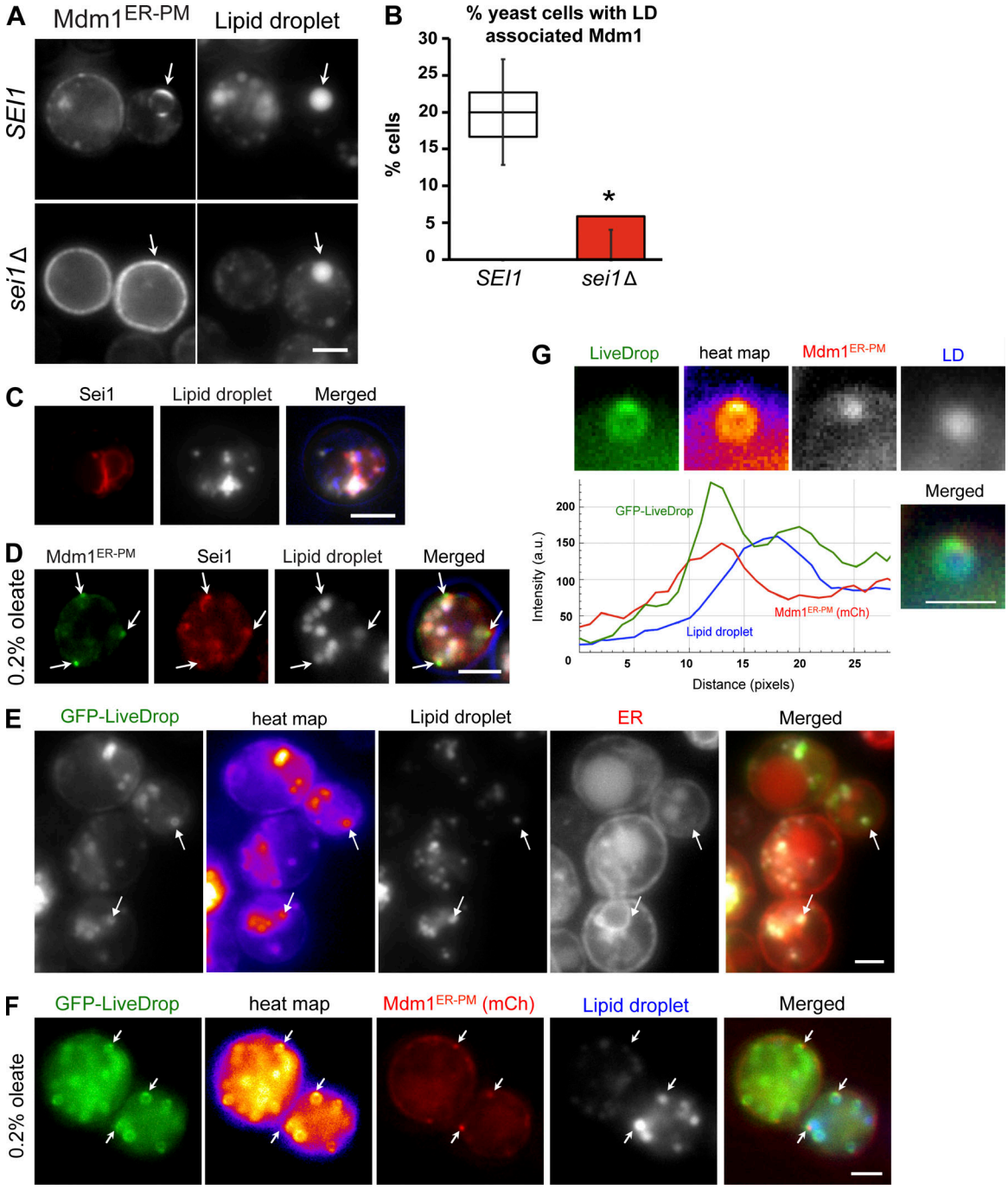

Figure S2. **Mdm1 colocalizes with LDs at ER–LD interfaces. (A)** Light microscopy of WT and seipin knockout (*sei1Δ*) yeast expressing Mdm1$^{ER\text{-}PM}$. LDs (gray) were visualized by using MDH. Arrows indicate the Mdm1-LD association in WT but not in *sei1Δ* yeast. Scale bar, 2 µm. **(B)** Quantification of Mdm1-associated LDs from images in A. Data represent the number of Mdm1-associated LDs over the total number of LDs; mean ± SD; $n > 50$ cells; *, $P < 0.01$; Student's *t* test. **(C)** Light microscopy of WT yeast expressing endogenously tagged Sei1 (tdTomato). LDs (gray) were visualized by using MDH. Scale bar, 2 µm. **(D)** Light microscopy of WT yeast expressing endogenously tagged Sei1 (tdTomato) and overexpressing GFP-tagged Mdm1$^{ER\text{-}PM}$ fed with 0.2% oleate. LDs (gray) were visualized by using MDH. Arrows indicate the colocalization of Sei1 and Mdm1$^{ER\text{-}PM}$ at LD bud sites. Scale bar, 2 µm. **(E)** Light microscopy of WT yeast expressing GFP-LiveDrop (and heat map). LDs (gray) were visualized by using MDH. Ds-Red HDEL marker was used to label the ER. Arrows indicate the colocalization of LiveDrop and LDs at the ER. Scale bar, 2 µm. **(F)** Light microscopy of WT yeast coexpressing GFP-LiveDrop (and heat map) and mCherry-tagged Mdm1$^{ER\text{-}PM}$. LDs (gray) were visualized by using MDH. Arrows indicate the enrichment of Mdm1$^{ER\text{-}PM}$ foci with LiveDrop at the ER. Scale bar, 2 µm. **(G)** Higher magnification of cells in D. Light microscopy of WT yeast coexpressing GFP-LiveDrop (and heat map) and Mdm1$^{ER\text{-}PM}$. LDs (gray) were visualized by using MDH. Scale bar, 2 µm. Bottom left: Line tracing of light microscopy images.

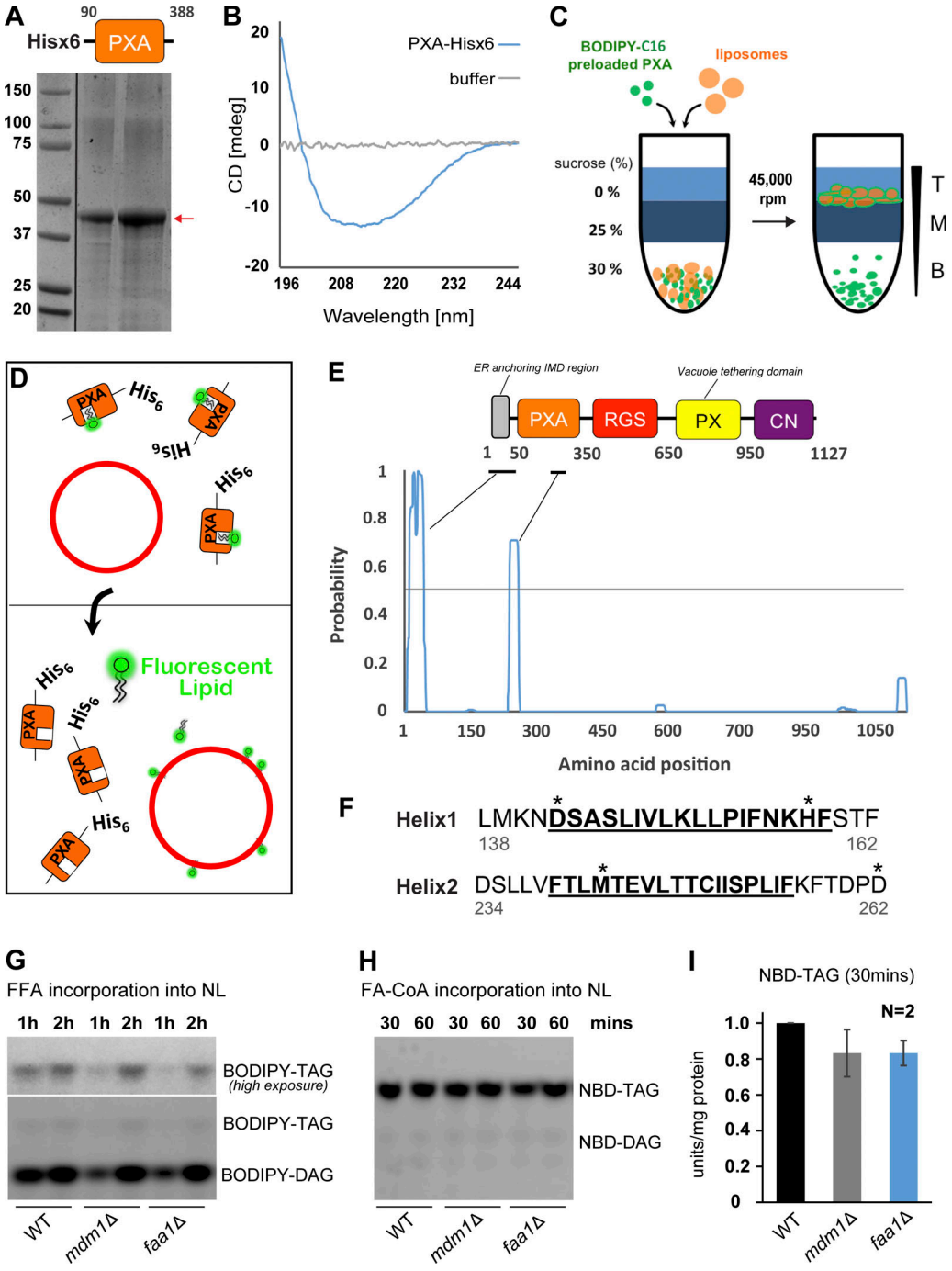

Figure S3. **The Mdm1 PXA domain is hydrophobic and binds FAs, and loss of Mdm1 perturbs FA activation. (A)** SDS-PAGE of yeast His-tagged PXA purified from *E. coli*. **(B)** Circular dichroism spectra of Hisx6-PXA and buffer only. **(C)** Diagram representing the flotation assay. T: Top fraction, M: Medium fraction, B: Bottom fraction. **(D)** Diagram describing the experiment in C and representing the anticipated outcome. **(E)** Hydrophobicity plot generated for Mdm1^{FL} by using Phobius. Top: Diagram representation of Mdm1 domains. Regions in the N-terminus and the PXA domain with high hydrophobicity probability are marked. RGS: regulator of G protein signaling, CN: C-terminal Nexin. **(F)** Amino acid sequence of PXA-Helix1 and PXA-Helix2. *, highly conserved amino acids. **(G)** TLC of BODIPY-C16 incorporation into BODIPY-DAG and -TAG in *mdm1Δ* and *faa1Δ* compared with WT yeast. Quantification in Fig. 4, F and G. NL, neutral lipid. **(H)** TLC of NBD-C16-CoA incorporation into NBD-TAG in *mdm1Δ* and *faa1Δ* compared with WT yeast. Quantification in Fig. 4 H. **(I)** Quantification of NBD-C16-CoA incorporation into NBD-TAG in *mdm1Δ* and *faa1Δ* relative to WT yeast (30-min incubation). *n* = 2. Raw data are shown in Fig. S3 H.

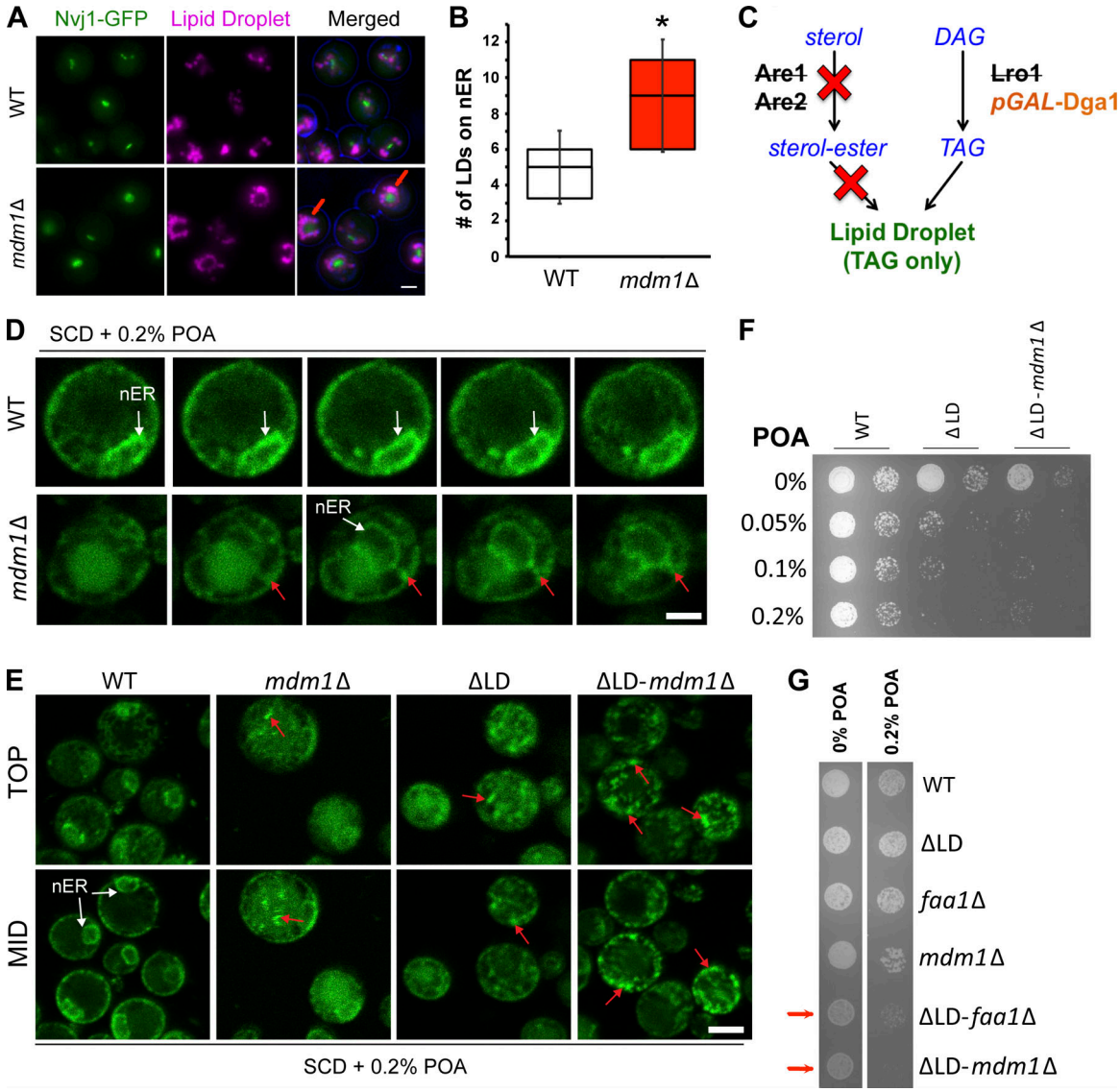

Figure S4. **Loss of Mdm1 sensitizes yeast to lipotoxic stress. (A)** Light microscopy of WT and Mdm1 knockout (*mdm1*Δ) yeast expressing Nvj1-GFP. LDs (magenta) were visualized by using MDH. Arrows indicate LDs at the nuclear envelope in *mdm1*Δ. Scale bar, 2 µm. **(B)** Quantification of the number of LDs on the nuclear envelope representing images in F. Data represent the number of LDs on the nuclear envelope over the total LDs; mean ± SD; $n > 50$ cells; *, $P < 0.01$; Student's *t* test. **(C)** Diagram depicting the genetic modifications made in the ΔLD yeast strain. **(D)** Slices from confocal microscopy of WT (top) and *mdm1*Δ (bottom) yeast fed 0.2% POA. ER (green) is marked by endogenous GFP-HDEL tagging. Red arrows indicate the deformed nuclear ER (nER) morphology and ER extensions in *mdm1*Δ yeast compared with WT. Scale bar, 0.5 µm. **(E)** Confocal microscopy of different yeast strains fed 0.2% POA. ER (green) is marked by endogenous GFP-HDEL tagging. Red arrows indicate the abnormal ER foci and tangles (nER: nuclear ER). Scale bar, 2 µm. **(F)** Plating assay for different yeast strains fed with varying amounts of POA and plated on SCD agar. **(G)** Plating assay for different yeast strains fed with varying amounts of POA and plated on SCD agar. Red arrows indicate strains that show pronounced sensitivity to POA.

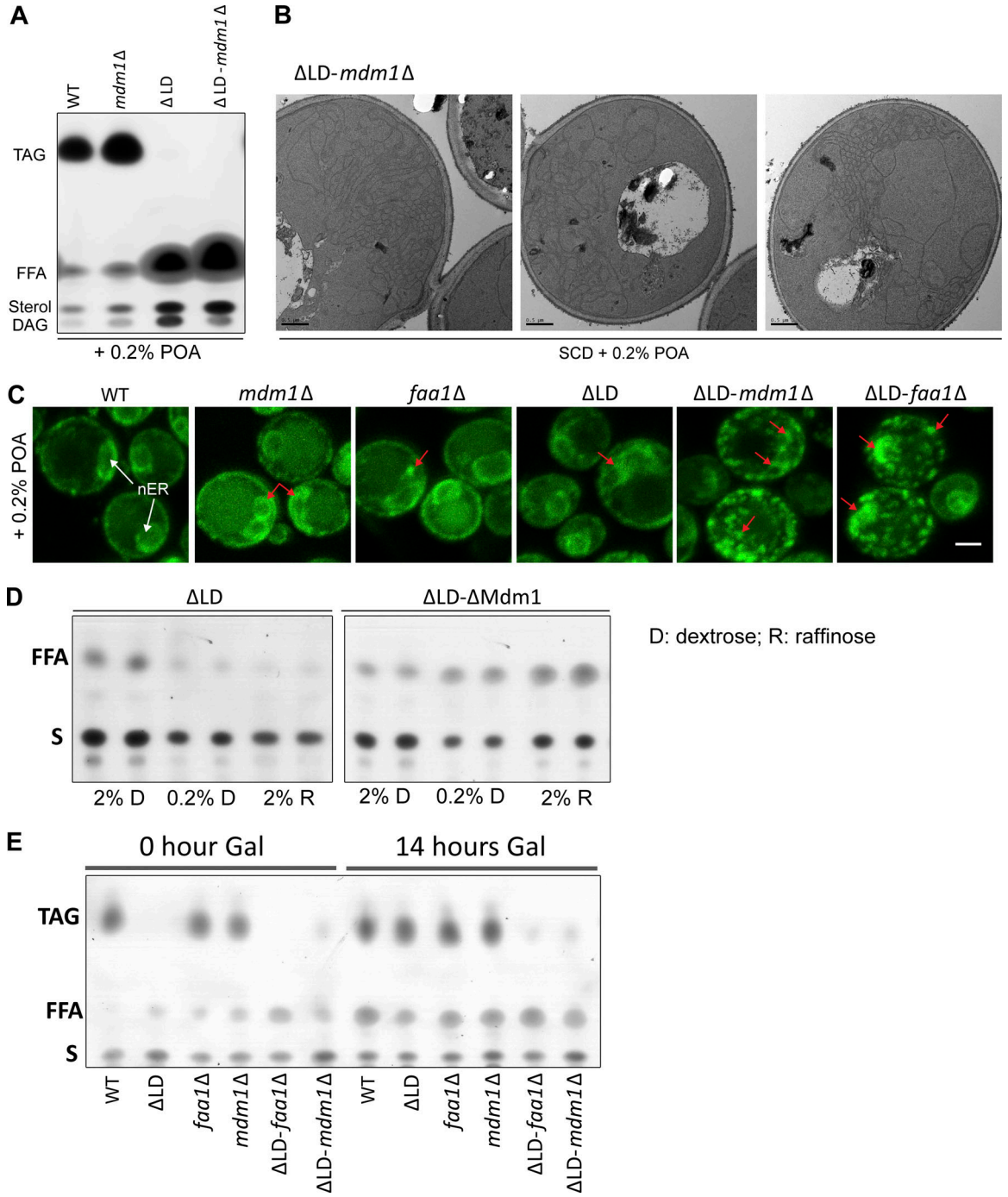

Figure S5. **Loss of Mdm1 perturbs TAG synthesis. (A)** TLC of neutral lipids extracted from yeast incubated in media containing 0.2% POA for 6 h. **(B)** Thin-sectioning TEM of ΔLD-*mdm1*Δ yeast fed 0.2% POA for 6 h showing extensive ER tubulations and deformed nuclear ER. Scale bar, 0.5 µm. **(C)** Confocal microscopy of different yeast strains fed 0.2% POA. ER (green) is marked by endogenous GFP-HDEL tagging. Red arrows indicate the abnormal ER foci and tangles (nER: nuclear ER). Scale bar, 2 µm. **(D)** TLC of neutral lipids extracted from ΔLD and ΔLD-*mdm1*Δ yeast incubated in different media. **(E)** TLC of neutral lipids extracted from different yeast strains extracted at 0 h and 14 h after galactose (Gal) induction.

Table S1. **List of yeast strains used in this study**

Strain	Genotype	Origin
SEY6210 (*WT*)	*MATα ura3-52 leu2-3,112 his3-Δ100 trp1-Δ901 lys2-801suc2-Δ9*	Scott Emr Lab[a]
Nvj1-GFP	*NVJ1-GFP::NATMX*	This study
Nvj1-mCherry	*NVJ1-MCHERRY::URA3*	This study
ss-DsRed-HDEL (ER marker)	*DSRED-HDEL::LEU2*	This study
mdm1Δ	*MDM1::KANMX*	Henne et al., 2015
Faa1-mCherry	*FAA1-MCHERRY::TRP1*	Hariri et al., 2018
sei1Δ	*SEI1:HYG*	This study
faa1Δ	*FAA1::HIS3*	This study
3.5KO (are1Δ are2Δ lro1Δ pGAL-DGA1)	*ARE1::HIS3 ARE2::LEU2 LRO1::URA3 TRP-GAL1-10(PROM) DGA1*	Choudhary et al., 2015
3.5KO (are1Δ are2Δ lro1Δ pGAL-DGA1) mdm1Δ	*ARE1::HIS3 ARE2::LEU2 LRO1::URA3 TRP-GAL1-10(PROM) DGA1 MDM1:KANMX*	This study
3.5KO (are1Δ are2Δ lro1Δ pGAL-DGA1) faa1Δ	*ARE1::HIS3 ARE2::LEU2 LRO1::URA3 TRP-GAL1-10(PROM) DGA1 FAA1:KANMX*	This study

Strains are in SEY6210 background unless otherwise noted.
[a]Scott Emr Lab, Weill Institute for Cell and Molecular Biology, Cornell University, Ithaca, NY.

Table S2. **Yeast expression plasmids used in this study**

Plasmid	Characteristics	Origin
Mdm1-mCherry	FL Mdm1-GFP with GPD promoter on pBP73G (Ura)	Hariri et al., 2018
Mdm1-GFP	FL Mdm1-GFP with GPD promoter on pBP73G	Henne et al., 2015
Mdm1-GFP R823E	Mdm1 FL with PX lipid binding mutation on pGP73G	Henne et al., 2015
$Mdm1^{1\text{-}PXA}$-GFP	Mdm1 N-terminal IMD and PXA (res 1–389) domains on pGP73G	Henne et al., 2015
$Mdm1^{IMD}$-GFP	Mdm1 IMD domain (1–51) on pGP73G	Henne et al., 2015
GFP alone	GFP on pGP73G	Henne et al., 2015
$Mdm1^{Tcb2\text{-}PXA}$-GFP	Tcb2 N-term (1–121)-Mdm1 PXA domain-GFP on pGP73G	This study
Mdm1 PXA-GFP	GFP-Soluble Mdm1 PXA domain on pGP73G	This study
Mdm1 PX+CN	GFP-Mdm1 PX+C-Nexin on pGP73G	This study
$Mdm1^{ER\text{-}PM}$	Mdm1 (1–389)-GFP-Ist2 polybasic region (877–946) on pGP73G	This study
$Mdm1^{ER\text{-}PM}$ (mCherry)	Mdm1 (1–389)-mCherry-Ist2 polybasic region (877–946) on pGP73G	This study
mini-$Mdm1^{ER\text{-}PM}$	Mdm1 IMD(1n51)-GFP-Ist2 polybasic region (877–946) on pGP73G	This study
$Mdm1^{Tcb2\ ER\text{-}PM}$	Tcb2(1–121)-Mdm1 PXA-GFP-Ist2 polybasic region (877–946) on pGP73G	This study
$Nvj1^{ER\text{-}PM}$	Nvj1 (1–120)-GFP-Ist2 polybasic region (877–946) on pGP73G	This study
GFP-LiveDrop	GFP-$GPAT4^{160\text{-}216}$ of *D.m.* GPAT4 on pGP73G	This study, adapted from Wang et al., 2016
GFP-PXA-Helix1	Mdm1 (138–162) on pGP73G	This study
GFP-PXA-Helix2	Mdm1 (234–262) on pGP73G	This study
SUMO-hisx6	*E. coli* plasmid pET28a	This study
PXA(129-264)-SUMO-hisx6 (*O. latipes*)	PXA in *E. coli* plasmid pET28a	This study
PXA(90-388)-hisx6 (*S. cerevisiae*)	Mdm1 PXA in *E.coli* plasmid pET23d	This study
GST	GST encoded in pGEX-6P-1	Henne et al., 2012
ss-GFP-HDEL (ER marker)	Plasmid with TPI(prom)-SS-GFP-HDEL for ER labeling with GFP	A kind gift from J. Friedman and Laura Lackner[a]

[a]J. Friedman, Dept. of Cell Biology, University of Texas Southwestern Medical Center, Dallas, TX. L. Lackner, Northwestern University, Dept. of Molecular Biosciences, Evanston, IL.

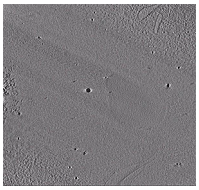

Video 1. **Tomographic reconstruction of ΔLD-*mdm1*Δ yeast represented in Fig. 5 D.**

References

Choudhary, V., N. Ojha, A. Golden, and W.A. Prinz. 2015. A conserved family of proteins facilitates nascent lipid droplet budding from the ER. *J. Cell Biol.* 211: 261–271. https://doi.org/10.1083/jcb.201505067

Hariri, H., S. Rogers, R. Ugrankar, Y.L. Liu, J.R. Feathers, and W.M. Henne. 2018. Lipid droplet biogenesis is spatially coordinated at ER-vacuole contacts under nutritional stress. *EMBO Rep.* 19:57–72. https://doi.org/10.15252/embr.201744815

Henne, W.M., N.J. Buchkovich, Y. Zhao, and S.D. Emr. 2012. The endosomal sorting complex ESCRT-II mediates the assembly and architecture of ESCRT-III helices. *Cell.* 151:356–371. https://doi.org/10.1016/j.cell.2012.08.039

Henne, W.M., L. Zhu, Z. Balogi, C. Stefan, J.A. Pleiss, and S.D. Emr. 2015. Mdm1/Snx13 is a novel ER-endolysosomal interorganelle tethering protein. *J. Cell Biol.* 210:541–551. https://doi.org/10.1083/jcb.201503088

Wang, C.-W., Y.-H. Miao, and Y.-S. Chang. 2014. A sterol-enriched vacuolar microdomain mediates stationary phase lipophagy in budding yeast. *J. Cell Biol.* 206:357–366. https://doi.org/10.1083/jcb.201404115

Wang, H., M. Becuwe, B.E. Housden, C. Chitraju, A.J. Porras, M.M. Graham, X.N. Liu, A.R. Thiam, D.B. Savage, A.K. Agarwal, et al. 2016. Seipin is required for converting nascent to mature lipid droplets. *eLife.* 5:5. https://doi.org/10.7554/eLife.16582